DOI: https://doi.org/10.37434/tpwj2022.10.02

EFFECT OF EXTERNAL ELECTROMAGNETIC FIELD CONFIGURATION ON METAL STRUCTURE OF WELDED JOINTS OF STRUCTURAL STEEL

O.D. Razmyshlyaev[1], **S.Yu. Maksymov**[2], **O.M. Berdnikova**[2], **O.O. Prylypko**[2], **O.S. Kushnaryova**[2], **T.O. Alekseyenko**[2]

[1]Pryazovskyi State Technical University
7 Universytetska Str., 87500, Mariupol, Ukraine
[2]E.O. Paton Electric Welding Institute of the NASU
11 Kazymyr Malevych Str., 03150, Kyiv, Ukraine

ABSTRACT

The peculiarities of metal structure of welded joints of structural low-alloy steel after welding using external electromagnetic field were studied. The phase composition, microstructure and microhardness of metal of welded joints produced without and with the use of alternating magnetic fields — longitudinal or transverse were studied. The structural parameters in the metal of the welds and areas of the heat-affected zone were analyzed. The conditions for producing high-quality welded joints during welding of low-alloy steels under the effect of external electromagnetic field, which provide strengthening and crack resistance of the metal, were found.

KEYWORDS: structural low-alloy steel, welded joints, external electromagnetic effect, alternating magnetic fields, heat-affected zone, phase composition, microstructure, microhardness

INTRODUCTION

Requirements to quality and reliability of welded joints are growing continuously. The need to expand the range of steels at welding led to development of the scientific direction of application of the external electromagnetic effect (EEE) on the weld pool melt for intensification of the processes of its degassing, lowering of hydrogen content, structure refining, improvement of the value of weld strength and ductility. Experimental studies allowed demonstrating the validity of theoretical conclusions on EEF effectiveness for lowering the weld metal proneness to pore formation, and the degassing mechanism formed under EEE impact, promotes reaching a high degree of homogeneity of fine porosity. In order to define it more precisely, it is necessary to determine the nature of distribution of the electric current lines in the weld pool, taking into account the conditions of welding. On this base it becomes possible to establish the optimum EEE parameters and to perform inductor calculations. The latter had to be made so as to generate magnetic induction exactly in the active part of the weld pool, i.e. in the region of an effective interaction of electric current and external electromagnetic field that causes melt displacement [1–3].

Solving the urgent problem of improvement of the effectiveness of consumable electrode arc surfacing and welding with the action of controlling magnetic fields, will allow increasing the productivity of the process of electrode wire melting, effectiveness of controlling the depth and width of the deposited beads, effectiveness of stirring of the weld pool liquid metal.

In arc welding longitudinal magnetic (LMF) and transverse magnetic (TMF) fields are used. In the first the induction vector is parallel, and in the second it is normal to the electrode and arc axis [3, 4].

Calculations were used to determine the values of the speed and acceleration reached by the liquid metal under the impact of alternating EEE, as well as optimum values of LMF and TMF induction and frequency that ensure effective stirring of the melt along the entire length of the pool at arc surfacing [5–10]. However, nothing is known about the influence of LMF and TMF on the structure which forms in the metal of the welds and in the HAZ.

The objective of this work is establishing the regularities of the influence of alternating EEE (LMF, TMF) on the structure and phase composition, microhardness and microstructure of welded joints of low-alloy structural 09G2S steel.

MATERIAL AND PROCEDURES

As a result of welding structural low-alloy 09G2S steel (14 mm thick) by Sv-08A filler wire (3 mm diameter) (AN-348 flux) welded joints were obtained with and without EEE application in the following modes: current I = 360 A; arc voltage U = 30–32 V; welding speed v = 30 m/h, reverse polarity, using flux-copper backing. Joint type was S4 (GOST 8713–78).

Table 1. Width (μm) of welded joint HAZ sections

HAZ subzones	Welded joints		
	Without EEE	LMF	TMF
I	1000–1600	1000–1600	1600–2200
II	1000	1200	1600
III	600	1000	1400
IV	600	800	1000

EEE was created by an inductor placed on the holder of the mechanism feeding the flux-cored wire, coaxially with it. Powered by alternating current of industrial frequency, the inductor generated an alternating magnetic field which permeated the liquid metal weld pool. Magnetic induction in the zone of the weld pool was equal to 20–25 mT. Three variants of welded joints were produced: without EEE application; with application of LMF (f = 2 Hz) and TMF (f = 6 Hz).

Microstructural studies were performed by light microscopy methods (Neophot-32 and Versamet-2 microscopes, Japan). Vickers hardness was measured in M-400 hardness meter (Leco Company, USA) at 0.1 kg load.

RESULTS AND THEIR DISCUSSION

In welded joints base metal (BM), weld metal, fusion line (FL), and HAZ were studied in the following regions: I — overheated (coarse grain); II — normalized (total recrystallization); III — incomplete recrystallization; IV — recrystallized. Structures of ferrite F, pearlite P, grain size D_{gr}, crystallite width h_{cr}, ferrite interlayer thickness δ(F) and *HV* microhardness were studied.

It was found that LMF and TMF affect the size of HAZ zones (Table 1). In the studied welded joints at EEE application the width of HAZ subzones becomes larger (Table 1) that is associated with the nature of liquid metal movement in the weld pool under EEE impact and features of metal heating and cooling.

Structure of 09G2S steel BM is ferritic-pearlitic at D_{gr} (F) = 10–20 μm, D_{gr} (P) = 40–80 μm and *HV* = = 1650–1760 (Figure 1, *a*). Structure of weld metal in all the joints is also ferritic-pearlitic (F–P) (Figure 1, *b–d*).

In the center of the metal of the weld without EEE the size (width) of pearlite crystallites is equal to h_{cr} (P) = 140–340 μm (Figure 1, *b*) at *HV* (P) = 2060 MPa, and the width of ferrite grain is h_{cr} (F) = 40–100 μm and *HV*(F) = 1810–1870 MPa. In the weld root h_{cr} (P) and h_{cr} (F) are equal to 60–100 μm. On FL, similar to the weld root, a slight lowering of microhardness was achieved, compared to the weld center — by 130 and 110–170 MPa, respectively.

Studies of the sample with LMF application showed that the width of F–P crystallites in the weld metal structure is equal to: h_{cr} (P) = 100–160 μm (Figure 1, *c*) at *HV*(P) = 1990–2080 MPa; h_{cr} (F) = 40–100 μm at *HV* (F) = 1760–1930 MPa. In the weld = root h_{cr} (P) = 60–140 μm and h_{cr} (F) = 20–40 μm. On FL h_{cr} (P) = 60–140 μm and h_{cr} (F) = 20–40 μm with a slight increase of microhardness, compared with the weld center: *HV*(P) = 1990–2280 MPa, *HV*(F) = = 1680–1990 MPa. Note that in the welded joint with LMF application in FL zone, i.e. at transition from the weld metal to HAZ I, a large cold crack of 1600 μm length formed (Figure 1, *e*).

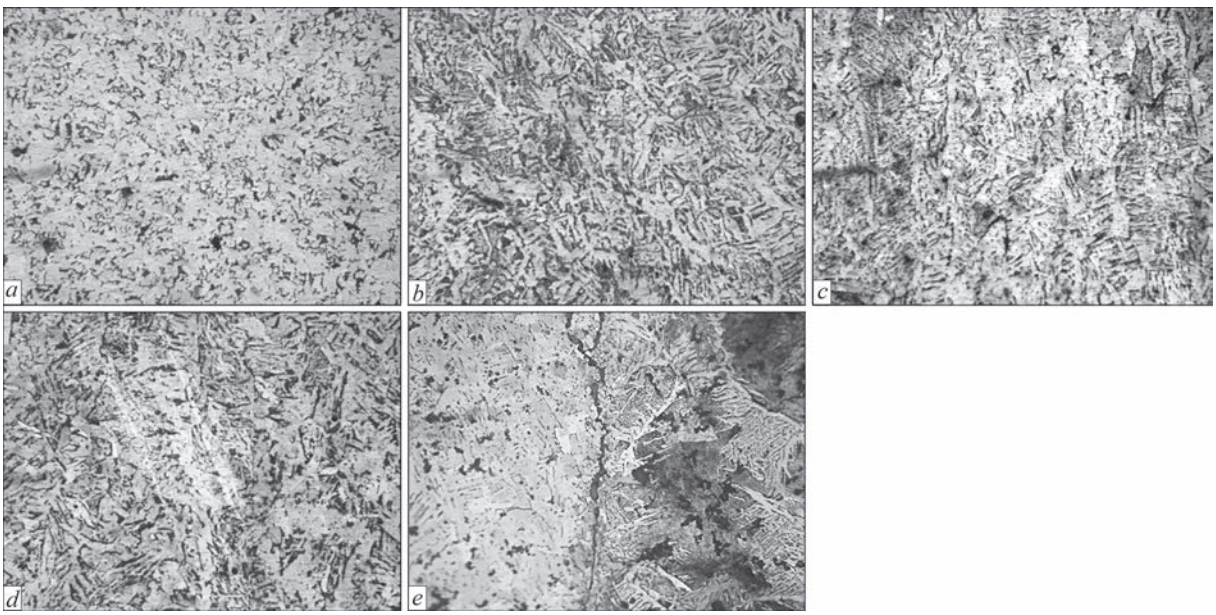

Figure 1. Microstructure (×250) of welded joints of 09G2S steel: *a* — BM; *b–d* — weld metal; *e* — FL, produced without EEE (*b*), with application of LMF (*c*, *e*) and TMF (*d*)

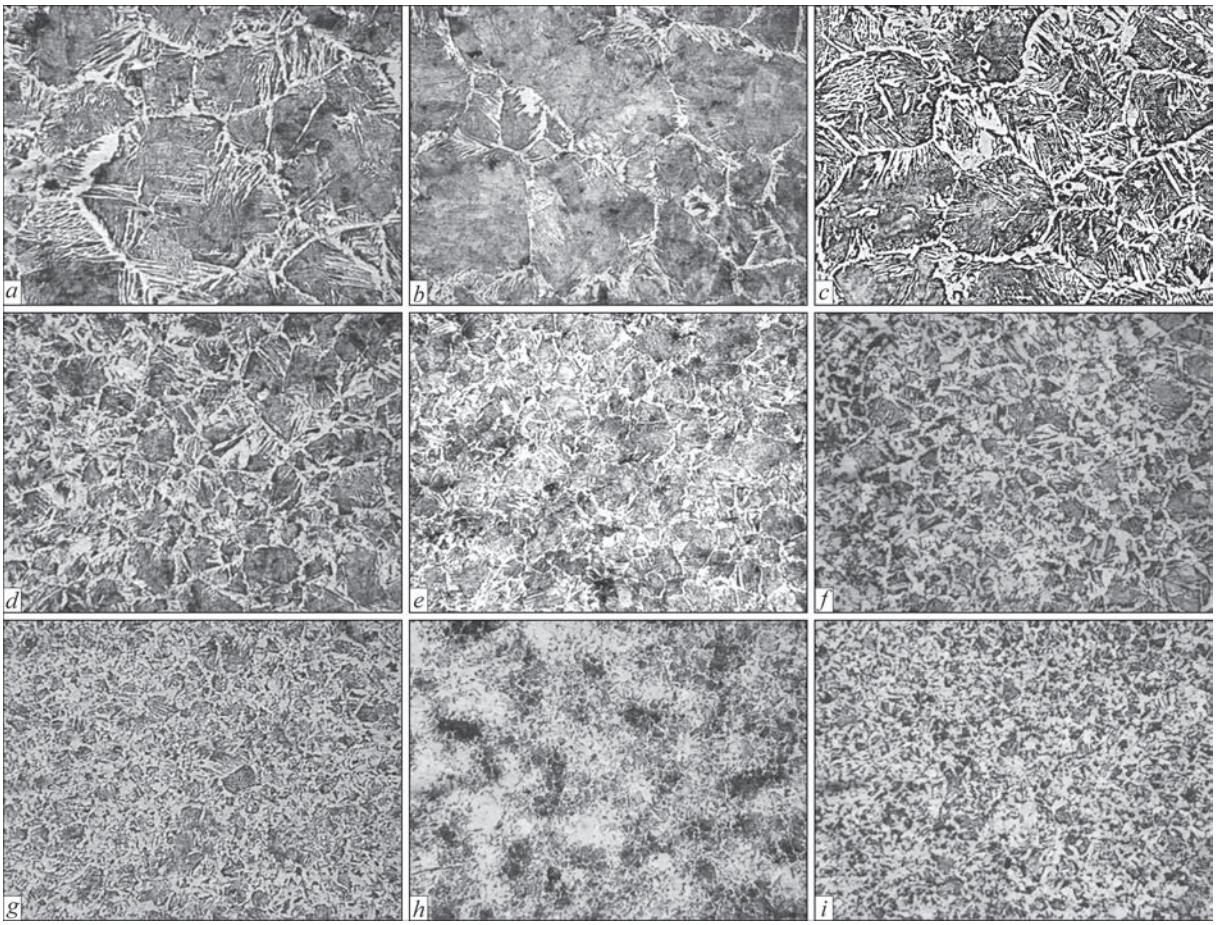

Figure 2. Microstructure (×250) of HAZ metal of 09G2S steel welded joints in subzones: *a–c* — HAZ I; *d–f* — HAZ II; *g–i* — HAZ III, IV obtained without EEE (*a*, *d*, *g*) with application of LMF (*b*, *e*, *h*) and TMF (*c*, *f*, *i*)

Investigations of a sample with TMF application revealed that the width of the crystallites in the weld metal h_{cr} (P) = 100–200 μm (Figure 1, *d*) at *HV* (P) = = 1930 MPa, and the width of ferrite grains — h_{cr} (F) = 20–60 μm at *HV*(F) = 1600–1760 MPa. In the weld root and on FL grain size h_{cr} (P) = 60–220 μm and h_{cr}(F) = 40–140 μm at *HV*(P) = 1930–2060 MPa, *HV*(F) = 1600–1760 MPa.

Investigations of the HAZ metal of welded joints (Figure 2) showed in HAZ I of a sample without EEE a pearlite structure with size D_{gr} (P) = 100–360 μm and interlayers of ferrite δ(F) = 30–70 μm at *HV* (P) = 2130–2210 MPa (Figure 2, *a*), *HV* (F) = 1810–1990 MPa. In HAZ II the structure is refined to D_{gr} (F–P) = 30–80 μm, microhardness is practically unchanged (*HV* (P) = 2060 MPa; *HV* (F) = 1870–1930 MPa) (Figure 2, *d*). In HAZ III, IV D_{gr} (F–P) = 10–50 μm at *HV* (F–P) = = 1810–1930 MPa (Figure 2, *g*).

Investigations of a sample with LMF application revealed formation in HAZ I of P-structure with size D_{gr} (P) = 140–340 μm and interlayers of ferrite δ(F) = = 20–100 μm at *HV* (P) = 2130–2210 MPa (Figure 2, *b*), *HV* (F) = 2060 MPa. In HAZ II–IV the structure is noticeably refined to D_{gr} (F–P) = 30–100 μm (HAZ II, Figure 2, *d*); D_{gr} (F–P) = 10–40 μm (HAZ III, Figure 2, *e*) and D_{gr} (F–P) = 20–80 μm (HAZ IV). In HAZ zone II the microhardness practically corresponds to that in HAZ I at its further lowering in HAZ III, IV to *HV* (F–P) = 1700–1930 MPa.

At TMF application in HAZ I, a pearlite structure forms with D_{gr} (P) = 100–280 μm and interlayers of ferrite δ (F) = 20–50 μm (Figure 2, *c*) at *HV* (P) = 1990–2060 MPa, *HV* (F) = 1760–1930 MPa. In HAZ II a fine-grained structure (D_{gr} (F–P) = 20–70 μm (Figure 2, *f*)) forms, microhardness decreases slightly (*HV* (P) = 1870–1990 MPa; *HV* (F) = 1760–1810 MPa). In HAZ III, IV the structure is refined to D_{gr} (F–P) = 10–70 μm (Figure 2, *i*) at *HV* (F–P) = = 1700–1870 MPa (HAZ III) and *HV* (F–P) = 1760–1930 MPa (HAZ IV) at *HV* (F–P) = 1810–1930 MPa.

Comparison of *HV* (Figure 3) and microstructure (Figure 4) parameters of the studied samples revealed the following. In a sample produced without EEE, a noticeable *HV* increase is observed in HAZ I and II compared to weld metal (Figure 3, *a*). In a sample with LMF application (Figure 3, *b*), an increase of *HV* is observed near FL from the weld side and in HAZ I, compared to a sample without EEE. Here, Δ*HV* gradient is equal to 320 MPa. It can cause cracking with further brittle fracture of the welded joint. The most

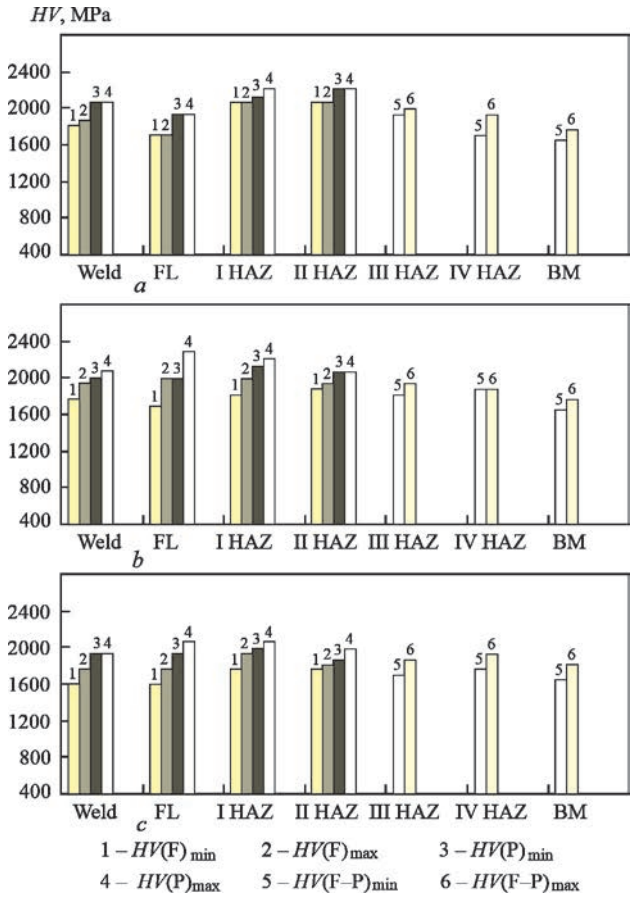

Figure 3. Microhardness (*HV*) of the metal of welded joints of 09G2S steel produced without EEE (*a*), with application of LMF (*b*) and TMF (*c*)

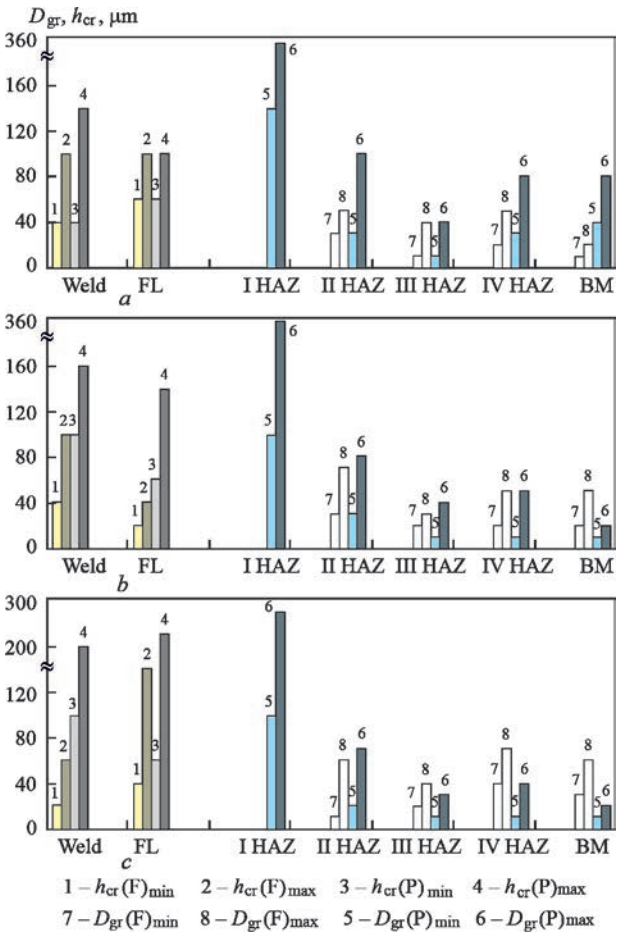

Figure 4. Structural parameters of the metal of 09G2S steel welded joints produced without EEE (*a*), with application of LMF (*b*) and TMF

uniform *HV* level both in the weld metal and in the HAZ, is observed in the welded joint produced with TMF application (Figure 3, *c*).

At application of LMF and TMF the grain structure in the welded joints is slightly coarsened in the weld metal near FL, compared to a sample without EEE (Figure 4). At transition to the HAZ, the structure is refined; slightly at LMF application and to a greater extent at TMF. Here, the width of ferrite interlayers at TMF decreases by 1.4 and 1.7 times on average, compared to samples without EEE or LMF. Moreover, at TMF application in HAZ I and II the grain is refined 1.3 times on average, compared to a sample without EEE. Such a dispersion of the structure will ensure both the strength, and higher fracture toughness of the metal and welded joint crack resistance, respectively. It should be also noted that EEE influence on the structural changes is the most evident in such local areas of welded joints and FL and HAZ I, and II.

Thus, it was established that the impact of EEE, in particular, of LMF and TMF, affects the HAZ dimensions, microstructure and microhardness of the metal of welds and HAZ, and crack formation in welded joints of low-alloy 09G2S steel.

At LMF application a coarse-grained structure forms, microhardness gradients are observed and cracks appear in FL zone. It can cause further brittle fracture of the welded joint.

TMF application ensures grain structure refinement in the overheated (HAZ I) and normalized (HAZ II) subzones, uniform level of microhardness, both in the weld metal, and in the HAZ subzones. Such structural changes will provide the strength, will improve the fracture toughness of the metal and will ensure cracking resistance of the welded joint, respectively.

CONCLUSIONS

1. In arc welding the impact of alternating magnetic fields affects the microhardness, microstructure parameters of welded joint metal and HAZ dimensions.

2. In welding low-alloy steel, the impact of external electromagnetic field is manifested to a greater extent in the zone of FL and HAZ in overheated (coarse-grain) and normalized (complete recrystallization) zones.

3. After application of the longitudinal magnetic field in FL zone, formation of a coarse-grain structure

at microhardness gradients led to cracking. It can be the cause of further brittle fracture of the welded joint.

4. Application of a transverse magnetic field ensured formation of the most favourable structure of welded joint metal at uniform level of microhardness, both in the weld metal, and in the HAZ subzones, and marked refinement of the structure in overheated (HAZ I) and normalized (HAZ II) zones. Such structural changes will both ensure the strength, and improve the fracture toughness of metal and crack resistance of the welded joint, respectively.

5. In welding low-alloy steel under EEE impact, the most effective is application of transverse magnetic fields, in which the induction vector is normal to the electrode and arc axes.

REFERENCES

1. Ryzhov, R.N., Kuznetsov, V.D., Prilipko, E.A. (2005) Calculation procedure of controlling electromagnetic effect parameters in arc welding of structural steels. *Vestnik HTUU KPI*, **45**, 176–177 [in Russian].
2. Ryzhov, R.N., Kuznetsov, V.D. (2006) External electromagnetic effects in the processes of arc welding and surfacing (Review). *The Paton Welding J.*, **10**, 36–44.
3. Ryzhov, R.N., Kuznetsov, V.D. (2005) Choice of optimal parameters of external electromagnetic action in arc methods of welding. *The Paton Welding J.*, **6**, 27–31.
4. Ryzhov, R.N. (2007) Influence of electromagnetic actions on process of formation and solidification of welds. *Svarochn. Proizvodstvo*, **2**, 56–58 [in Russian].
5. Ahieieva, A.D. (2019) Rational using of the controlling longitudinal and transverse magnetic fields at arc welding and surfacing. *IOP Conf. Series: Mater. Sci. and Engin*.
6. Ageeva, M.V., Razmyshlyaev, A.D. (2019) Influence of combined magnetic field on wire melting rate in arc surfacing. *Tekhnichni Nauky ta Tekhnologii*, 18(**4**), 22–27 [in Russian].
7. Boldyrev, A.M., Birzhev, V.A., Chernykh, A.V. (1992) To calculation of hydrodynamic parameters of liquid metal on welding pool bottom in arc welding. *Svarochn. Proizvodstvo*, **2**, 31–33 [in Russian].
8. Boldyrev, A.M., Birzhev, V.A., Martynenko, A.I. (2008) Examination of influence of variable axial magnetic field on process of electrode wire melting. *Svarochn. Proizvodstvo*, **2**(6–8), 63, 64 [in Russian].
9. Mironova, M.V. (2013) To choice of optimal schemes of input devices of transverse magnetic field for processes of arc welding and surfacing. In: *Zbirnyk Nauk. Prats of DSTU, Tekhnichni Nauky*, 21(**1**), 74–78 [in Russian].
10. Lazarenko, M.A., Razmyshlyaev, A.D. (2000) Structure of controlling magnetic fields for welding and surfacing processes using the devices with cylindrical 304 symmetry. *Visnyk PDTU*, **9**, 160–163 [in Russian].

ORCID

S.Yu. Maksymov: 0000-0002-5788-0753,
O.M. Berdnikova: 0000-0001-9754-9478,
O.O. Prylypko: 0000-0001-5244-5624,
O.S. Kushnaryova: 0000-0002-2125-1795,
T.O. Alekseyenko: 0000-0001-8492-753X

CONFLICT OF INTEREST

The Authors declare no conflict of interest

CORRESPONDING AUTHOR

S.Yu. Maksymov
E.O. Paton Electric Welding Institute of the NASU
11 Kazymyr Malevych Str., 03150, Kyiv, Ukraine.
E-mail: maksimov@paton.kiev.ua

SUGGESTED CITATION

O.D. Razmyshlyaev, S.Yu. Maksymov, O.M. Berdnikova, O.O. Prylypko, O.S. Kushnaryova, T.O. Alekseyenko (2022) Effect of external electromagnetic field configuration on metal structure of welded joints of structural steel. *The Paton Welding J.*, **10**, 13–17.

JOURNAL HOME PAGE

https://pwj.com.ua/en

Received: 29.08.2022
Accepted: 01.12.2022